ACADEMIC
PRESS

Available online at www.sciencedirect.com
SCIENCE DIRECT®

Journal of Solid State Chemistry 172 (2003) 194–199

JOURNAL OF
SOLID STATE
CHEMISTRY

http://elsevier.com/locate/jssc

Synthesis and characterization of mixed metal organic–inorganic hybrid compounds with a pillared layer structure: $CuVO_2(4,4'\text{-bpy})(XO_4)$ (X=P, As)

Chih-Min Wang[a] and Kwang-Hwa Lii[a,b,*]

[a] Department of Chemistry, National Central University, Chungli 320, Taiwan, ROC
[b] Institute of Chemistry, Academia Sinica, Nankang, Taipei 115, Taiwan, ROC

Received 5 September 2002; received in revised form 12 November 2002; accepted 26 November 2002

Abstract

Two mixed metal organic–inorganic hybrid compounds, $CuVO_2(4,4'\text{-bpy})(PO_4)$, **1**, and $CuVO_2(4,4'\text{-bpy})(AsO_4)$, **2**, have been synthesized under hydrothermal conditions and structurally characterized by single-crystal X-ray diffraction. The two compounds are isostructural and crystallize in the monoclinic space group $C2/c$ (No. 15) with $a = 21.941(2)$ Å, $b = 8.0915(7)$ Å, $c = 15.856(1)$ Å, $\beta = 110.424(2)^\circ$, $Z = 8$, and $R_1 = 0.037$ for **1**, and $a = 21.923(2)$ Å, $b = 8.2447(9)$ Å, $c = 16.176(2)$ Å, $\beta = 110.967(2)^\circ$, $Z = 8$, and $R_1 = 0.041$ for **2**. The structure consists of bimetallic oxide layers covalently linked through 4,4′-bpy pillars into a 3D framework. Each oxide layer is constructed from corner-sharing VO_4 and PO_4 tetrahedra and CuN_2O_3 square pyramids. On the basis of magnetic susceptibility study of **1**, bond-valence calculation and the presence of dioxovanadium unit, the Cu atom is divalent and the V atom is pentavalent.

Keywords: Copper; Vanadium; Phosphate; Arsenate; Bipyridine

1. Introduction

The synthesis of organic–inorganic hybrid open-framework materials has been a subject of intense research owing to their interesting structural chemistry and potential applications in ion exchange, adsorption and catalysis [1–4]. A common approach for the design of such materials is the use of metal centers coordinated to multidentate rigid ligands containing N- or/and O-donor atoms. Open-framework metal phosphates have grown to be one of the largest family of inorganic solids synthesized during the last decade or so [5]. Recently, many researchers have used a new approach to the synthesis of open-framework materials in which phosphate is mixed with a bidentate organic ligand. It has been established that oxalate readily substitutes for phosphate in the skeletons of inorganic phosphates forming oxalate–phosphate hybrid compounds with channels similar to those found in zeolites [6–19]. Three different types of oxalate coordination are observed in these structures, namely, bisbidentate, monobidentate, and bismono- and bisbidentate. Another interesting variant of the metal phosphate is obtained by incorporating 4,4′-bipyridine in the structure. A good number of compounds in the 4,4′-bpy-phosphate system have been reported during the last few years [20–25]. In their structures, the 4,4′-bpy unit can act either as a monoprotonated pendant ligand or as a neutral bridging ligand. For example, $[Ga_4(4,4'\text{-Hbpy})(PO_4)(H_{0.5}PO_4)_2(HPO_4)_2(H_2PO_4)_2(H_2O)_2]\cdot H_2O$, which contains monoprotonated pendant 4,4′-Hbpy, is unique in such a way that among the vast number of synthetic phosphates and naturally occurring phosphate minerals it is the first example in which four different types of monophosphate are present in the same structure [21]. $[Ni(4,4'\text{-bpy})_2(H_2PO_4)_2]\cdot C_4H_9OH\cdot H_2O$ exhibits a new type of interpenetration involving a 2D square net and a rarely observed 3D $CdSO_4$-type framework of the same chemical composition [22]. $[(VO_2)_2(4,4'\text{-bpy})_{0.5}(4,4'\text{-Hbpy})(PO_4)]\cdot H_2O$ has a layer structure with the

---

*Corresponding author. Institute of Chemistry, Academia Sinica, Nankang, Taipei 115, Taiwan, ROC. Fax: +886-3-4227664.
E-mail address: liikh@cc.ncu.edu.tw (K.-H. Lii).

0022-4596/03/$ - see front matter © 2003 Elsevier Science (USA). All rights reserved.
doi:10.1016/S0022-4596(03)00021-5

monoprotonated 4,4′-Hbpy ligand being coordinated to vanadium (V) as a pendent group [23]. $NH_4[(V_2O_3)_2(4,4'\text{-bpy})_2(H_2PO_4)(PO_4)_2]\cdot 0.5H_2O$ consists of layers of mixed-valence vanadium (IV,V) phosphate pillared through 4,4′-bpy ligands into a 3D structure [24]. It is the first mixed-valence compound in the 4,4′-bpy-phosphate system. The 3D structures of the mixed metal compounds $M(VO_2)_2(4,4'\text{-bpy})_2(HPO_4)_2$ ($M=$ Co, Ni, Cu) contain 2D layers of metal phosphate linked by neutral 4,4′-bpy pillars [25]. We have now synthesized a new member in the family, $CuVO_2(4,4'\text{-bpy})(PO_4)$, **1**, and the arsenate analogue $CuVO_2(4,4'\text{-bpy})(AsO_4)$, **2**, which are similar to $M(VO_2)_2(4,4'\text{-bpy})_2(HPO_4)_2$ in composition, but adopt a considerably different structure. The synthesis and structural characterization of the two compounds are reported.

2. Experimental section

2.1. Synthesis and initial characterization

The hydrothermal reactions were carried out in Teflon-lined stainless-steel Parr acid digestion bombs. All chemicals were purchased from Aldrich. Arsenic acid was prepared from a reaction of As_2O_3 and H_2O_2. Reaction of V_2O_5 (0.10 mmol), $Cu(NO_3)_2\cdot 3H_2O$ (0.25 mmol), 4,4′-bipyridine (2 mmol), H_3PO_4 (8 mmol), and H_2O (10 mL) in a Teflon-lined acid digestion bomb at 180°C for 3 d produced blue tablet crystals of $CuVO_2(4,4'\text{-bpy})(PO_4)$, **1**. The pH values before and after the reaction were 3.0 and 2.1, respectively. The product was filtered, washed with water, rinsed with ethanol, and dried in a desiccator. The yield was 90% based on vanadium. Powder X-ray diffraction pattern of the bulk product is in good agreement with the calculated pattern based on the results from single-crystal X-ray diffraction (Fig. 1). The disparate peak intensity of the first reflection with respect to other peaks suggests a preferential orientation of the crystallites in a planar manner. Energy-dispersive X-ray fluorescence spectroscopy of several blue crystals confirms the presence of Cu, V and P. Elemental analysis results of the bulk product are consistent with the stoichiometry of **1**. Anal. found: C, 29.99%; H, 2.04%; N, 6.85%. Calcd: C, 30.20%; H, 2.03%; N, 7.05%. We have also carried out retro-syntheses and used the stoichiometric ratio of 1:1:1:1 (Cu:V:bpy:P); the resulting products are a mixture of **1** and a significant amount of unidentified brown side-product. Blue tablet crystals of $CuVO_2(4,4'\text{-bpy})(AsO_4)$, **2**, were synthesized under similar reaction conditions. The yield was 93% based on vanadium. The bulk product is monophasic as indicated by powder X-ray diffraction. Anal. found: C, 27.09%; H, 1.79%; N, 6.18%. Calcd: C, 27.20%; H, 1.83%; N, 6.35%.

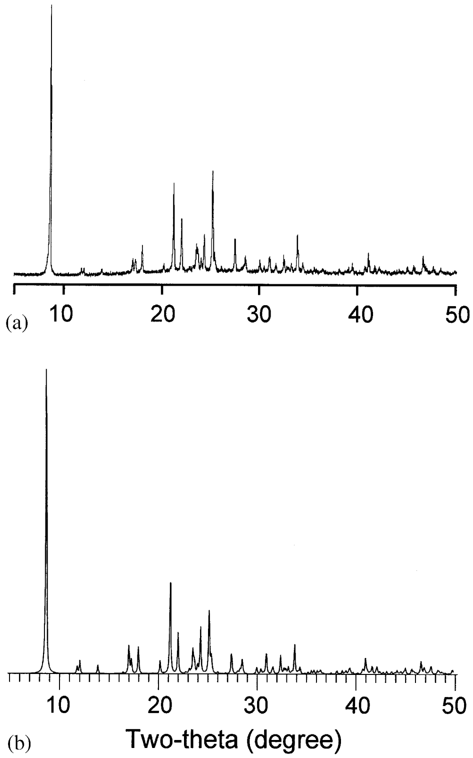

Fig. 1. (a) X-ray powder pattern of **1**. (b) Simulated powder pattern from the atomic coordinates derived from single-crystal X-ray diffraction.

2.2. Magnetic susceptibility measurements

Variable-temperature magnetic susceptibility $\chi(T)$ data were obtained on 42.2 mg of polycrystalline sample of **1** from 2 to 300 K in a magnetic field of 5000 G after zero-field cooling using a SQUID magnetometer. Correction for diamagnetism was made according to Selwood [26].

2.3. Single-crystal X-ray diffraction

A suitable crystal of each compound was selected for indexing and intensity data collection on a Siemens SMART CCD diffractometer equipped with a normal focus, 3-kW sealed tube X-ray source. Intensity data were collected at room temperature in 1271 frames with ω scans (width 0.30° per frame). Empirical absorption corrections based on symmetry equivalents were applied. The structures were solved by direct methods and difference Fourier syntheses. Bond-valence calculation results indicate V atoms are pentavalent [27]. The H atoms, which are bonded to C atoms in 4,4′-bpy molecule, were positioned geometrically and refined using a riding model with fixed isotropic thermal parameters. The final cycles of least-squares refinement included atomic coordinates and anisotropic thermal parameters for all non-hydrogen atoms. All calculations were performed using the SHELXTL Version 5.1 software package [28].

Table 1
Crystallographic data for $CuVO_2$(4,4′-bpy)(PO_4) (**1**) and $CuVO_2$(4,4′-bpy)(AsO_4) (**2**)

	1	**2**
Crystal size (mm)	$0.34 \times 0.09 \times 0.04$	$0.18 \times 0.08 \times 0.04$
Crystal system	Monoclinic	Monoclinic
Space group	*C*2/*c* (no. 15)	*C*2/*c* (no. 15)
a (Å)	21.941(2)	21.923(2)
b (Å)	8.0915(7)	8.2447(9)
c (Å)	15.856(1)	16.176(2)
β (deg)	110.424(2)	110.967(2)
V $(\text{Å})^3$	2638.0(7)	2730.3(8)
Z	8	8
*F*w	397.63	441.58
T (K)	296	296
λ(Mo*K*α) (Å)	0.71073	0.71073
ρ_{calc} (g/cm^3)	2.002	2.149
μ(Mo*K*α) (cm^{-1})	24.7	46.7
$T_{\text{min, max}}$	0.733/0.961	0.738/0.957
$2\theta_{\text{max}}$ (deg.)	56.5	56.6
Unique data ($I > 2\sigma(I)$)	2329	2694
No. of variables	190	190
R_1[a]	0.0372	0.0414
wR_2[b]	0.1083	0.1087
$(\Delta\rho)_{\text{max, min}}$	1.14, −0.39	1.18, −0.88

[a] $R_1 = \sum|F_o| - |F_c| / \sum|F_o|$.

[b] $wR_2 = \sum\left\{\left[w(F_o^2 - F_c^2)^2\right] / \sum\left[w(F_o^2)^2\right]\right\}^{1/2}$, $w = 1/[\sigma^2(F_o^2) + (aP)^2 + bP]$, $P = [\max(F_o, 0) + 2(F_c)^2]/3$, where $a = 0.0610$ and $b = 0$ for **1** and $a = 0.0581$ and $b = 2.07$ for **2**.

3. Results and discussion

3.1. Magnetic susceptibility

Fig. 2 shows the inverse magnetic susceptibility of **1** plotted as a function of temperature. The data from 2 to 300 K were well described by the equation $\chi_M = C/(T - \theta)$ where $C = 0.522\,\text{cm}^3\,\text{K/mol}$ and $\theta = -2.78\,\text{K}$. From the equation, $C = N\mu_{\text{eff}}/3k_B$, one obtains the effective magnetic moment μ_{eff} per formula unit = 2.04 BM, which confirms the presence of one unpaired electron per formula unit and is consistent with the observations that the magnetic moments of simple Cu^{II} complexes are generally in the range from 1.75 to 2.20 BM.

3.2. Description of the structure

The crystallographic data, atomic coordinates and selected bond lengths for **1** and **2** are given in Tables 1, 2 and 3, respectively. The two compounds are isostructural and crystallize in the monoclinic space group *C*2/*c* with a unit cell content of eight formula units. All atoms are at general positions. On the basis of magnetic susceptibility study of **1**, bond-valence calculation and the presence of dioxovanadium unit (vide infra), the Cu atom is divalent and the V atom is pentavalent. The 4,4′-bpy molecule is coordinated to two Cu atoms as a bridging ligand. Fig. 3 shows the coordination environments of Cu and V atoms in the structure. The d^9 configuration makes Cu^{II} subject to Jahn–Teller distortion. The Cu atom is 5-coordinate in a geometry of square pyramid. There is a planar array of four short Cu–O(or N) bonds (1.924–2.012 Å for **1** and 1.924–2.013 Å for **2**) and a very long Cu–O(5) bond (2.449 Å in **1** and 2.505 Å in **2**). The distortion is so drastic that the Cu atom may be regarded as 4-coordinate. The two N atoms from two 4,4′-bpy ligands are in *trans* positions. The oxygen atom, O(5), has a small field strength and prefers the positions with the stretched bond at the apical position because it forms a very short V–O distance corresponding effectively to formation of a vanadyl (V=O) group by $p\pi$ donation from oxygen to vacant $3d\pi$-orbitals on vanadium. Each V^{5+} cation has a distorted tetrahedral coordination in which two positions are occupied by doubly bonded oxygen atoms (O(5) and O(6)) and the remaining positions are occupied by two PO_4^{3-} anions. The tetrahedral arrangement with two very short V=O bonds is a feature characteristic of vanadium (V). Each phosphate ligand coordinates to two Cu and two V atoms. The 4,4′-bpy molecule is not planar and the two pyridyl rings are twisted at an angle of 38.9°. The distance between neighboring 4,4′-bpy molecules along the *b*-axis is 4.0 Å. The two rings are twisted to introduce attractive intermolecular edge-to-face aromatic interaction. The structure is termed an "edge-tilted-T" [29]. The shortest carbon-to-carbon distance between adjacent 4,4′-bpy molecules in the *ac* plane is 3.75 Å.

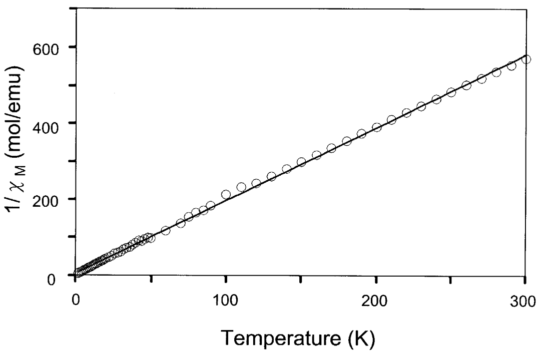

Fig. 2. $1/\chi_M$ versus T for a powder sample of **1**.

As shown in Fig. 4a, the structure of **1** consists of bimetallic oxide layers covalently linked through 4,4′-bpy pillars into a 3D framework. Thus, the structure exhibits the characteristic pattern of alternating organic/inorganic domains often observed in metal organopho-

Table 2
Atomic coordinates and thermal parameters for $CuVO_2$(4,4′-bpy)(PO_4) (**1**) and $CuVO_2$(4,4′-bpy)(AsO_4) (**2**)[a]

Atom	x	y	z	U_{eq}[b]
Compound **1**				
Cu(1)	0.26545(2)	0.73170(6)	0.20946(3)	0.0165(1)
V(1)	0.17161(3)	0.11852(8)	−0.08071(4)	0.0196(2)
P(1)	0.27113(5)	0.0521(1)	0.12248(6)	0.0162(2)
O(1)	0.2072(1)	0.0825(3)	0.0412(2)	0.0279(6)
O(2)	0.3242(1)	0.1578(3)	0.1033(2)	0.0306(7)
O(3)	0.2908(1)	−0.1283(3)	0.1265(2)	0.0190(5)
O(4)	0.2621(1)	0.1034(4)	0.2081(2)	0.0291(7)
O(5)	0.2098(1)	0.0114(5)	−0.1352(2)	0.0271(6)
O(6)	0.0954(1)	0.0673(4)	−0.1188(2)	0.0329(7)
N(1)	0.3550(2)	0.7501(4)	0.3006(2)	0.0198(7)
N(2)	0.6729(2)	0.7665(4)	0.6236(2)	0.0196(7)
C(1)	0.3658(2)	0.8165(5)	0.3819(2)	0.0210(8)
C(2)	0.4268(2)	0.8188(5)	0.4482(2)	0.0221(8)
C(3)	0.4053(2)	0.6862(5)	0.2830(2)	0.0260(9)
C(4)	0.4678(2)	0.6847(5)	0.3452(2)	0.0257(9)
C(5)	0.4796(2)	0.7535(5)	0.4308(2)	0.0215(8)
C(6)	0.5464(2)	0.7575(5)	0.4979(2)	0.0212(8)
C(7)	0.5587(2)	0.7302(5)	0.5892(3)	0.029(1)
C(8)	0.6218(2)	0.7363(5)	0.6492(3)	0.0282(9)
C(9)	0.5996(2)	0.7990(5)	0.4718(2)	0.0220(8)
C(10)	0.6614(2)	0.7930(5)	0.5358(2)	0.0216(8)
Compound **2**				
Cu(1)	0.26421(2)	0.72032(6)	0.20560(3)	0.0160(1)
V(1)	0.16913(3)	0.12193(9)	−0.08153(4)	0.0168(2)
As(1)	0.27187(2)	0.04339(5)	0.12338(3)	0.0154(1)
O(1)	0.2010(2)	0.0867(4)	0.0388(2)	0.0294(8)
O(2)	0.3298(2)	0.1573(4)	0.1041(2)	0.0328(8)
O(3)	0.2922(2)	−0.1503(4)	0.1230(2)	0.0178(6)
O(4)	0.2651(2)	0.0860(4)	0.2187(2)	0.0303(8)
O(5)	0.2106(2)	0.0232(4)	−0.1308(2)	0.0276(7)
O(6)	0.0936(2)	0.0662(4)	−0.1230(2)	0.0312(8)
N(1)	0.3532(2)	0.7417(4)	0.2976(2)	0.0192(8)
N(2)	0.6712(2)	0.7708(4)	0.6203(2)	0.0192(8)
C(1)	0.3633(2)	0.8132(6)	0.3759(3)	0.0205(9)
C(2)	0.4242(2)	0.8188(6)	0.4426(3)	0.0225(9)
C(3)	0.4042(2)	0.6758(6)	0.2835(3)	0.025(1)
C(4)	0.4668(2)	0.6788(6)	0.3459(3)	0.027(1)
C(5)	0.4778(2)	0.7519(5)	0.4276(3)	0.0210(9)
C(6)	0.5446(2)	0.7585(5)	0.4946(3)	0.0200(9)
C(7)	0.5566(2)	0.7328(6)	0.5855(3)	0.028(1)
C(8)	0.6200(2)	0.7408(6)	0.6449(3)	0.026(1)
C(9)	0.5976(2)	0.7904(6)	0.4704(3)	0.0225(8)
C(10)	0.6599(2)	0.7952(6)	0.5342(3)	0.0202(9)

[a] The coordinates of hydrogen atoms are given in supplementary materials.

[b] U_{eq} is defined as one-third of the trace of the orthogonalized U_{ij} tensor.

Table 3
Bond lengths (Å) for $CuVO_2$(4,4′-bpy)(PO_4) (**1**) and $CuVO_2$(4,4′-bpy)(AsO_4) (**2**)[a]

Compound **1**			
Cu(1)–O(3)^{ii}	1.958(2)	Cu(1)–O(4)^{iii}	1.924(2)
Cu(1)–N(1)	1.998(3)	Cu(1)–N(2)^{iv}	2.012(3)
Cu(1)–O(5)	2.449(2)	V(1)–O(1)	1.838(2)
V(1)–O(2)^{i}	1.853(3)	V(1)–O(5)	1.644(3)
V(1)–O(6)	1.621(3)	P(1)–O(1)	1.558(3)
P(1)–O(2)	1.559(3)	P(1)–O(3)	1.517(3)
P(1)–O(4)	1.498(2)	N(1)–C(1)	1.341(5)
N(1)–C(3)	1.332(5)	N(2)–C(8)	1.343(5)
N(2)–C(10)	1.342(5)	C(1)–C(2)	1.384(5)
C(2)–C(5)	1.388(5)	C(3)–C(4)	1.382(5)
C(4)–C(5)	1.404(5)	C(5)–C(6)	1.482(5)
C(6)–C(7)	1.394(5)	C(6)–C(9)	1.391(5)
C(7)–C(8)	1.379(6)	C(9)–C(10)	1.382(5)
Compound **2**			
Cu(1)–O(3)^{ii}	1.972(3)	Cu(1)–O(4)^{iii}	1.924(3)
Cu(1)–N(1)	1.993(4)	Cu(1)–N(2)^{iv}	2.013(4)
Cu(1)–O(5)	2.505(3)	V(1)–O(1)	1.841(3)
V(1)–O(2)^{i}	1.858(3)	V(1)–O(5)	1.626(3)
V(1)–O(6)	1.615(3)	As(1)–O(1)	1.701(3)
As(1)–O(2)	1.696(3)	As(1)–O(3)	1.659(3)
As(1)–O(4)	1.639(3)	N(1)–C(1)	1.342(6)
N(1)–C(3)	1.334(6)	N(2)–C(8)	1.343(6)
N(2)–C(10)	1.340(5)	C(1)–C(2)	1.385(6)
C(2)–C(5)	1.396(6)	C(3)–C(4)	1.385(6)
C(4)–C(5)	1.392(6)	C(5)–C(6)	1.479(6)
C(6)–C(7)	1.414(6)	C(6)–C(9)	1.378(6)
C(7)–C(8)	1.378(6)	C(9)–C(10)	1.386(6)

Symmetry codes: (i) $-x+1/2, -y+1/2, -z$; (ii) $x, y+1, z$; (iii) $-x+1/2, y+1/2, -z+1/2$; (iv) $x-1/2, -y+3/2, z-1/2$.

[a] The C–H bond lengths are 0.93 Å.

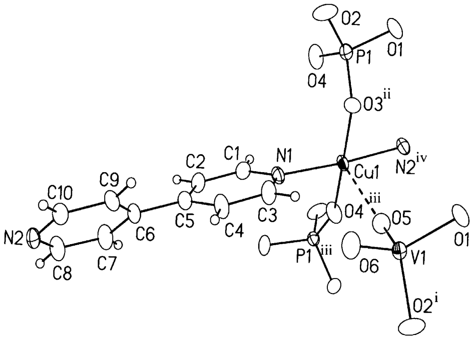

Fig. 3. The coordination environments of Cu and V in the structure of **1** showing atom labeling scheme. Thermal ellipsoids are shown at 50% probability. Small open circles represent hydrogen atoms. Dashed line represents the very long Cu–O bond. Symmetry codes: (i) $-x+1/2, -y+1/2, -z$; (ii) $x, y+1, z$; (iii) $-x+1/2, y+1/2, -z+1/2$; and (iv) $x-1/2, -y+3/2, z-1/2$.

sphonate phases [30]. Several other members in the 4,4′-bpy-phosphate system also adopt a pillared layer structure [20,24,25].

The oxide layer, shown in Fig. 4b, is constructed from corner-sharing {VO_4} and {PO_4} tetrahedra and {CuN_2O_3} square pyramids. Each 4,4′-bpy ligand tethers Cu sites in adjacent layers to produce a 1D $_{\infty}$[Cu(4,4′-bpy)] chain as a structural unit. Each PO_4 tetrahedron bridges two Cu atoms and two V atoms. Each VO_4 tetrahedron bridges two P atoms and one Cu atom, leaving one terminal *oxo* group, which is directed into the interlamellar region. The covalent connectivity in the layer produces four-membered {V_2P_2}, five-membered {Cu_2VP_2}, and six-membered

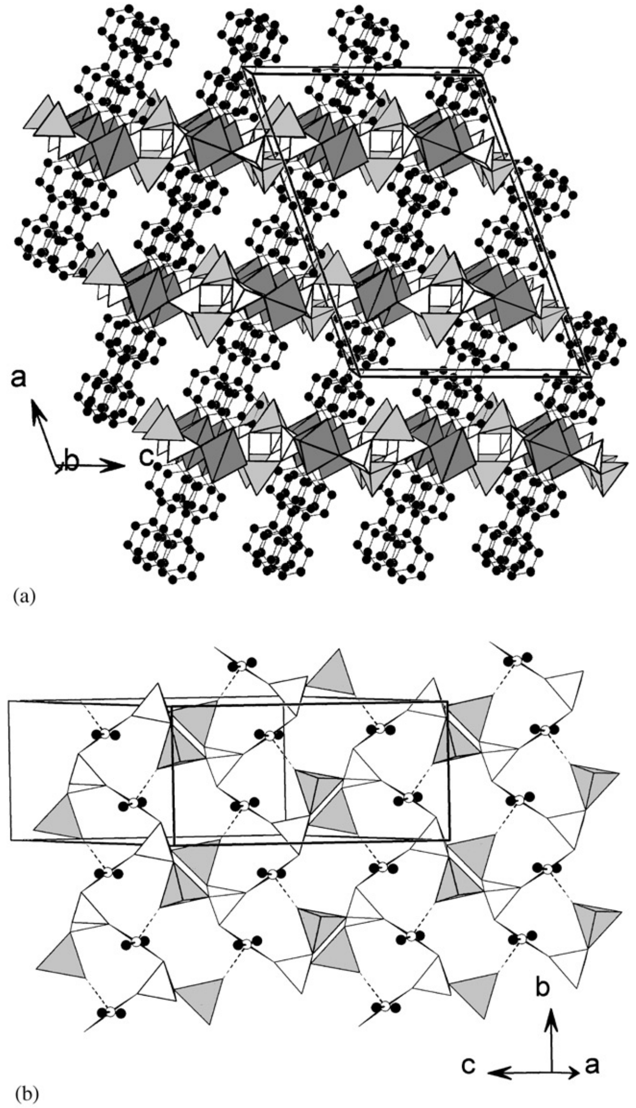

Fig. 4. (a) Structure of **1** viewed along the *b*-axis. The CuN_2O_3 square pyramids are shown in dark gray, VO_4 tetrahedra in light gray, and phosphate tetrahedra in white. Solid circles are N and C atoms. H atoms are not shown. (b) Section of an inorganic layer in **1** viewed in a direction approximately parallel to [101]. Ball-and-stick representation is used for CuN_2O_3 square pyramids. Circles with dot pattern and solid circles represent Cu and N atoms, respectively. Dashed lines represent the very long Cu–O bonds.

$\{Cu_2V_2P_2\}$ rings, which fuse to propagate the network structure.

During the course of the study of the Cu/V/4,4′-bpy/PO_4 system we synthesized another new compound. Green tablet crystals of $Cu(VO_2)_2$(4,4′-bpy)$_2$(HPO_4)$_2$ were obtained by heating a mixture of V_2O_5 (0.30 mmol), $Cu(NO_3)_2 \cdot 3H_2O$ (0.25 mmol), 4,4′-bpy (2 mmol), H_3PO_4 or H_3AsO_4 (8 mmol), and H_2O (10 mL) at 180°C for 3 d. Three times amount of V_2O_5 is used in this reaction than that for **1**. This compound has a smaller Cu content than **1**, and is isostructural with $M(VO_2)_2$(4,4′-bpy)$_2$(HPO_4)$_2$ (M = Co, Ni) [25]. The structure consists of trimers with the composition $MV_2O_4^{4+}$ (M = Co, Ni, Cu) that are connected by corner-sharing HPO_4^- tetrahedra to form 2D neutral layers with the composition $_\infty[MV_2O_4(HPO_4)_2]$, which are further linked through 4,4′-bpy pillars to generate a 3D framework. Within an oxide layer there are 10-sided windows formed by the edges of two MN_2O_4 octahedra, four VNO_4 trigonal bipyramids, and four phosphate tetrahedra. The 4,4′-bpy molecule is planar and is coordinated to one Cu (or Co, Ni) in a layer and one V atom in an adjacent layer as a bridging ligand. In contrast, the 4,4′-bpy molecule in **1** bridges two Cu atoms. Although the title compounds and $M(VO_2)_2$(4,4′-bpy)$_2$(HPO_4)$_2$ are similar in composition, they adopt considerably different structures.

We aim to combine the flexibility of metal organic coordination systems with the tetrahedral phosphate anions to produce new open-framework structures. The isolation of the 3D covalent framework material $CuVO_2$(4,4′-bpy)(PO_4) and its arsenate analogue illustrates once again that 4,4′-bipyridine molecule and phosphate (or arsenate) anion can be employed as structural building units in the synthesis of organic–inorganic hybrid compounds. They are the second examples of mixed metal compounds in the 4,4′-bpy-phosphate system and their structures can be described as metal phosphate layers pillared by 4,4′-bpy ligands. This type of structure is common and is seen in about one-half of the compounds in the system. It is evident that other factors such as solvent and the identity of counter cations contribute to the design of solid-state architectures. It is also interesting to explore mixed-valence materials (e.g., Fe^{II}/Fe^{III}) where the two metals have different coordination preferences and order on different crystallographic sites. Further work on these themes is in progress.

Acknowledgments

We thank the National Science Council for support, Ms. F.-L. Liao and Prof. S.-L. Wang at the National Tsing Hua University for X-ray data collection.

Supplementary materials

Crystallographic data for structures **1** and **2** reported in this paper have been deposited with the Cambridge Crystallographic Data Center as supplementary publication no. CCDC-196477 & 196478.

References

[1] P.J. Hagrman, D. Hagrman, J. Zubieta, Angew. Chem. Int. Ed. 38 (1999) 2638 (and references therein).

[2] G. Férey, Chem. Mater. 13 (2001) 3084 (and references therein).
[3] M. Eddaoudi, D.B. Moler, H. Li, B. Chen, T.M. Reineke, M. O'Keeffe, O.M. Yaghi, Acc. Chem. Res. 34 (2001) 319 (and references therein).
[4] M.E. Davis, Nature 417 (2002) 813 (and references therein).
[5] A.K. Cheetham, G. Férey, T. Loiseau, Angew. Chem. Int. Ed. 38 (1999) 3286 (and references therein).
[6] H.-M. Lin, K.-H. Lii, Y.-C. Jiang, S.-L. Wang, Chem. Mater. 11 (1999) 519.
[7] Z.A.D. Lethbridge, P. Lightfoot, J. Solid State Chem. 143 (1999) 58.
[8] A. Choudhury, S. Natarajan, C.N.R. Rao, J. Solid State Chem. 146 (1999) 538.
[9] A. Choudhury, S. Natarajan, J. Mater. Chem. 9 (1999) 3113.
[10] A. Choudhury, S. Natarajan, C.N.R. Rao, Chem. Eur. J. 6 (2000) 1168.
[11] W.-J. Chang, H.-M. Lin, K.-H. Lii, J. Solid State Chem. 157 (2000) 233.
[12] Y.-M. Tsai, S.-L. Wang, C.-H. Huang, K.-H. Lii, Inorg. Chem. 38 (1999) 4183.
[13] J. Do, R.P. Bontchev, A.J. Jacobson, Chem. Mater. 13 (2001) 2601.
[14] P. Lightfoot, Z.A.D. Lethbridge, R.E. Morris, D.S. Wragg, P.A. Wright, A. Kvick, G.B.M. Vaughan, J. Solid State Chem. 143 (1999) 74.
[15] C.-Y. Chen, P.P. Chu, K.-H. Lii, Chem. Commun. (1999) 1473.
[16] K.-H. Lii, C.-Y. Chen, Inorg. Chem. 39 (2000) 3374.
[17] L.-C. Huang, H.-M. Kao, K.-H. Lii, Chem. Mater. 12 (2000) 2411.
[18] Y.-F. Huang, K.-H. Lii, J. Chem. Soc. Dalton Trans. (1998) 4085.
[19] Z.A.D. Lethbridge, S.K. Tiwary, A. Harrison, P. Lightfoot, J. Chem. Soc. Dalton Trans. (2001) 1904.
[20] K.-H. Lii, Y.-F. Huang, Inorg. Chem. 38 (1999) 1348.
[21] C.-Y. Chen, F.-R. Lo, H.-M. Kao, K.-H. Lii, Chem. Commun. (2000) 1061.
[22] Y.-C. Jiang, Y.-C. Lai, S.-L. Wang, K.-H. Lii, Inorg. Chem. 40 (2001) 5320.
[23] L.-H. Huang, H.-M. Kao, K.-H. Lii, Inorg. Chem. 41 (2002) 2936.
[24] L.-I. Hung, S.-L. Wang, H.-M. Kao, K.-H. Lii, Inorg. Chem. 41 (2002) 3929.
[25] Z. Shi, S. Feng, S. Gao, L. Zhang, G. Yang, J. Hua, Angew. Chem. Int. Ed. 39 (2000) 2325 ($M(VO_2)_2(4,4'\text{-bpy})_2(HPO_4)_2$ ($M = $ Co, Ni)); C.-M. Wang, K.-H. Lii, unpublished research ($Cu(VO_2)_2(4,4'\text{-bpy})_2(HPO_4)_2$).
[26] P.W. Selwood, Magnetochemistry, Interscience, New York, 1956.
[27] I.D. Brown, D. Altermatt, Acta Crystallogr. B 41 (1985) 244.
[28] G.M. Sheldrick, SHELXTL Programs, version 5.1, Bruker AXS GmbH, Karlsruhe, Germany, 1998.
[29] W.B. Jennings, B.M. Farrell, J.F. Malone, Acc. Chem. Res. 34 (2001) 885.
[30] M.I. Khan, J. Zubieta, Prog. Inorg. Chem. 34 (1995) 1.